Planetary and Space Science 134 (2016) 122–127

Contents lists available at ScienceDirect

Planetary and Space Science

journal homepage: www.elsevier.com/locate/pss

FC colour images of dwarf planet Ceres reveal a complicated geological history

A. Nathues[a,*], M. Hoffmann[a], T. Platz[a], G.S. Thangjam[a], E.A. Cloutis[b], V. Reddy[a,c], L. Le Corre[a,c], J.-Y. Li[c], K. Mengel[d], A. Rivkin[e], D.M. Applin[b], M. Schaefer[a], U. Christensen[a], H. Sierks[a], J. Ripken[a], B.E. Schmidt[f], H. Hiesinger[g], M.V. Sykes[c], H.G. Sizemore[c], F. Preusker[h], C.T. Russell[i]

[a] Max Planck Institute for Solar System Research, Goettingen, Germany
[b] University of Winnipeg, Winnipeg, Canada
[c] Planetary Science Institute, Tucson, AZ, USA
[d] IELF, TU Clausthal, Clausthal-Zellerfeld, Germany
[e] Johns Hopkins University, Applied Physics Laboratory, USA
[f] Georgia Institute of Technology, Atlanta, GA, USA
[g] Institut für Planetologie, Westfälische Wilhelms Universität Münster, Germany
[h] German Aerospace Center, Institute of Planetary Research, Germany
[i] Institute of Geophysics and Planetary Physics, Department of Earth, Planetary and Space Sciences, University of California Los Angeles, Los Angeles, CA, USA

ARTICLE INFO

Keywords:
Asteroid
Ceres
Colour spectra
Imaging
Mineralogy
Surface

ABSTRACT

The dwarf planet Ceres (equatorial diameter 963km) is the largest object that has remained in the main asteroid belt (Russell and Raymond, 2012), while most large bodies have been destroyed or removed by dynamical processes (Petit et al. 2001; Minton and Malhotra, 2009). Pre-Dawn investigations (McCord and Sotin, 2005; Castillo-Rogez and McCord, 2010; Castillo-Rogez et al., 2011) suggest that Ceres is a thermally evolved, but still volatile-rich body with potential geological activity, that was never completely molten, but possibly differentiated into a rocky core, an ice-rich mantle, and may contain remnant internal liquid water. Thermal alteration should contribute to producing a (dark) carbonaceous chondritic-like surface (McCord and Sotin, 2005; Castillo-Rogez and McCord, 2010; Castillo-Rogez et al., 2011; Nathues et al., 2015) containing ammoniated phyllosilicates (King et al., 1992; De Sanctis et al., 2015 and 2016). Here we show and analyse global contrast-rich colour mosaics, derived from a camera on-board Dawn at Ceres (Russell et al., 2016). Colours are unexpectedly more diverse on global scale than anticipated by Hubble Space Telescope (Li et al., 2006) and ground-based observations (Reddy et al. 2015). Dawn data led to the identification of five major colour units. The youngest units identified by crater counting, termed bright and bluish units, are exclusively found at equatorial and intermediate latitudes. We identified correlations between the distribution of the colour units, crater size, and formation age, inferring a crustal stratigraphy. Surface brightness and spectral properties are not correlated. The youngest surface features are the bright spots at crater Occator (~Ø 92km). Their colour spectra are highly consistent with the presence of carbonates while most of the remaining surface resembles modifications of various types of ordinary carbonaceous chondrites.

1. Introduction

The Dawn spacecraft (Russell and Raymond, 2012) carries two Framing Cameras (FCs) which obtained images in seven colours (centre wavelength at 0.43, 0.55, 0.65, 0.75, 0.83, 0.92 and 0.98μm) and one clear filter ranging between 0.45 and 0.92μm (Sierks et al., 2012), mapping the surface of Ceres at ~140m/pixel during the High Altitude Mapping Orbit (HAMO), i.e., from ~1400km above the surface (Russell et al., 2016). Image mosaics, derived via applying image processing tools (Nathues et al., 2015; Reddy et al., 2012), are used to determine the global surface colour characteristics of Ceres. All colour mosaics, forming a global image cube, have been photometrically corrected by applying Hapke's photometric model (Hapke, 1981, 1999, 2012 and references therein) using iteratively derived light scattering parameters from Approach, Survey orbit and HAMO orbit imagery. Potential endogenic resurfacing processes such as cryovolcan-

* Corresponding author.
E-mail address: nathues@mps.mpg.de (A. Nathues).

http://dx.doi.org/10.1016/j.pss.2016.10.017
Received 8 July 2016; Received in revised form 14 October 2016; Accepted 31 October 2016
Available online 05 November 2016

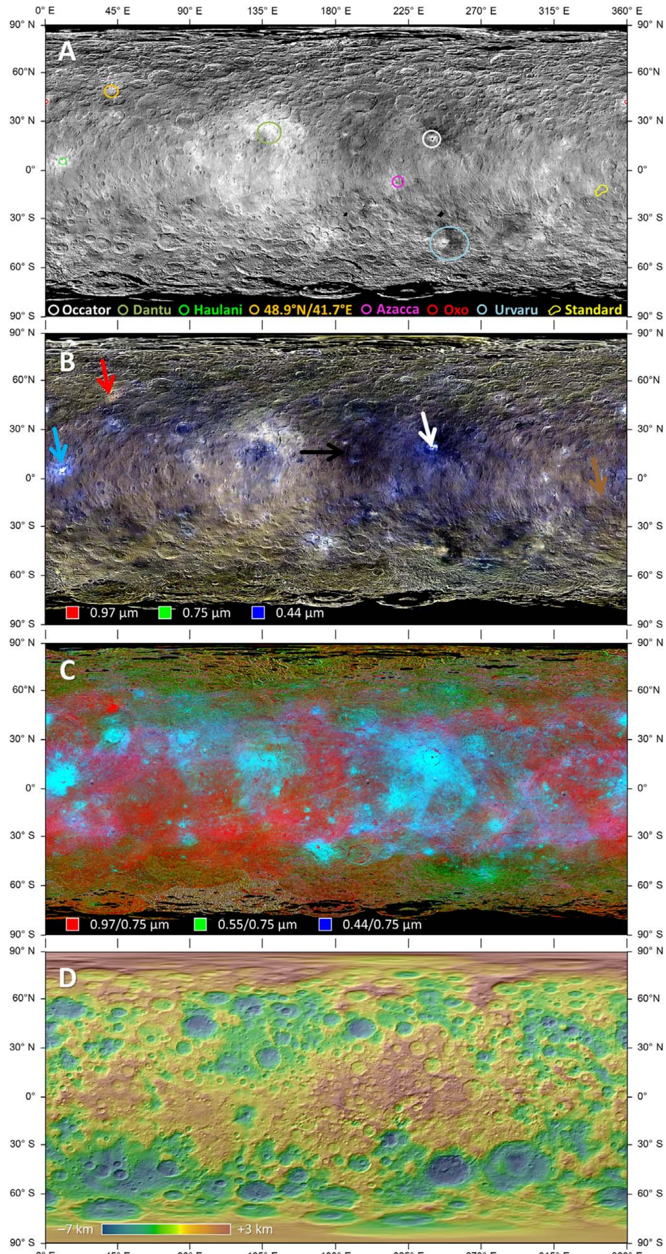

Fig. 1. Global Ceres mosaics in cylindrical projection. (A) Photometrically corrected HAMO clear filter mosaic showing albedo diversity and locations of investigated surface features. (B) RGB HAMO/Survey colour mosaic (Red=0.965µm, Green=0.749µm, Blue=0.438µm). Examples of identified colour units are marked by arrows. (C) Colour ratio Survey mosaic using Red=$R_{0.965\ \mu m}/R_{0.749\ \mu m}$, Green=$R_{0.555\ \mu m}$ /$R_{0.749\ \mu m}$, and Blue=$R_{0.438\ \mu m}/R_{0.749\ \mu m}$, where $R_{(\lambda)}$ is the reflectance in a specific filter. (D) Colour-coded topographic shaded relief map of Ceres with blue corresponding to the lowest elevation and red to the highest. Minimum and maximum elevations are computed relative to a 482×482×446km reference ellipsoid. (For interpretation of the references to color in this figure legend, the reader is referred to the web version of this article).

ism (e.g., Castillo-Rogez et al., 2011; Ruesch et al., 2016) as well as impact-induced tectonics (Hiesinger et al., 2016) have mainly shaped the cerean surface, forming a few large basins and a multitude of craters, of which some have been modified by viscous relaxation as indicated by crater morphology (see Fig. 1A). Surface areas retaining original primordial composition several million years after accretion and partial differentiation (e.g., Mc Cord and Sotin, 2005; Castillo-Rogez and Mc Cord, 2010) may not exist anymore due to resurfacing, or they are at least challenging to identify. The most pristine materials can probably be found at locations of the most recent, unweathered surfaces: fresh crater ejecta and exposed crater interior materials. We are going to show apparent correlations of the local geologic history with colour properties. One area where craters > 5km are absent, i.e., the surface is less modified by larger impacts but of older age, has been selected as our spectral standard site (Fig. S3D).

2. Surface colour units

The global clear filter mosaic (Fig. 1A) exhibits a large diversity of reflectances ranging between ~0.03 and 0.37; however most of the surface is on the lower end of this range. The darkest sites are associated with impact craters, for example, ejecta of Occator and Nawish, and floor material of Urvara, Yalode, and Ezinu. The brightest sites are located on the crater floors and rims of Occator, Oxo, Haulani, and Dantu.

Ceres' colours are more diverse than one could anticipate from ground-based observations (Larson et al., 1979; Rivkin et al., 2006; Li et al., 2006; Reddy et al., 2015), e.g., by the homogenous rotationally resolved spectra. Phenomenologically, we define five colour units (see Fig. 1B) on the basis of absolute reflectance, peak reflectance position, and spectral slopes. The identified units in order of decreasing reflectance are (reflectance values are measured at 0.653µm):

(1) Bright sites/spots: show highest reflectivities (up to 0.35), but can have spectra of different shape ranging from overall positively sloped to slightly negatively sloped longward of 0.653µm (Fig. 2A and B, Fig. S1). These sites cover a small part of Ceres' surface and

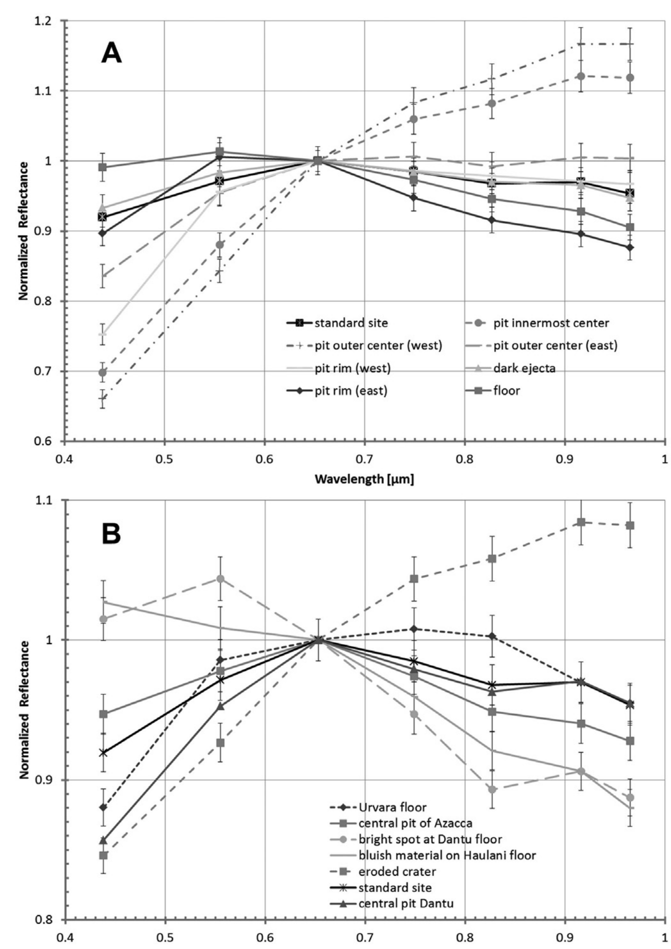

Fig. 2. Colour spectra of sites in Occator (A) and other craters (B). For comparison, the spectrum of our standard site is shown. Figure (A) shows mainly bright sites in Occator (cp. Fig. S1). Spectra are normalized to 0.653µm and error bars show standard deviation.

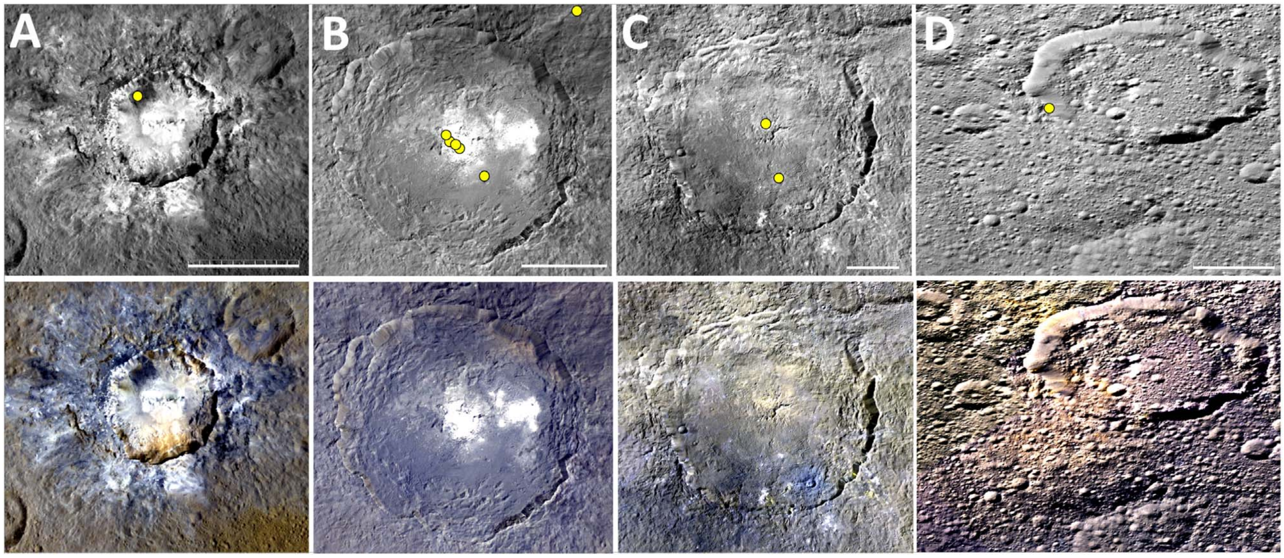

Fig. 3. Diverse colour units on Ceres. Upper panel images show reflectances in filter 0.555µm and lower panel images are RGB composite images of filters 0.965µm, 0.749µm, and 0.438µm. (A) Haulani (Ø 34km, 5.8°N/10.8°E) exhibiting bluish material as rayed ejecta. (B) Occator (crater Ø 92km, 19.8°N/239.3°E) containing the brightest sites ('spots'). (C) Dantu (Ø126km, 24.3°N/138.2°E) containing bluish material in the south and brownish material in the north. (D) Heavily degraded unnamed impact crater adjacent to Ernutet crater (lower left sub-image, Ø 54km, 48.9°N/41.7°E) containing unique dark reddish material. Symbols indicate the locations from which the respective colour spectra in Fig. 2 were taken. The scale bar length is 30km and north is up. (For interpretation of the references to color in this figure legend, the reader is referred to the web version of this article.)

exist mostly at crater floors and walls.

(2) Bluish sites: reflectivities range typically between 0.03 and 0.07, with a peak reflectance in FC filters at 0.438 or 0.555µm. (see Fig. 2B, Fig. S1, 'bluish material on Haulani floor'). This unit is most prevalent in and around craters of a particular size range and age (see below).

(3) Reddish site: A singular eroded crater (Fig. 3D) represents this small but distinct colour unit which is characterized by the steepest overall red spectral slope and reflectivities between 0.029 and 0.044 (cp. Fig. 2B, Fig. S1 'eroded crater'). The eroded crater is located close to Ernutet crater (diameter approx. 54 km).

(4) Brownish sites: characterized by low reflectances (0.025–0.035), whose reflectivity peaks at 0.653µm with concave down spectral shape (cp. Fig. 2, Fig. S1 'standard site'). Prevalent on the floors of large basins and areas apparently lacking young impacts.

(5) Dark sites: characterized by reflectances < 0.025. Spectral shapes are otherwise similar to bluish and brownish sites (cp. Fig. 2A, Fig. S1, 'dark ejecta'). Prevalent as ejecta fields of medium sized craters.

3. Prominent surface features

Occator (Fig. 3B) is the most prominent surface feature, exhibiting the largest reflectivity range and the brightest materials on Ceres (Nathues et al., 2015). It shows the highest spectral diversity and exhibits a dark ejecta field to its north-east. The central bright spot of Occator, a pit ~9km in diameter covered with bright material, shows signs of activity in the form of water ice sublimation (Küppers et al., 2014; Nathues et al., 2015), potential deposition of salts and clays (Nathues et al., 2015), and carbonates (De Sanctis et al., 2016). The pit exhibits at least three types of colour spectra: a) overall positively sloped spectra in the innermost centre and on some parts of the outer centre (Fig. 2A, 'pit innermost centre' and 'pit outer centre – west'); b) positively sloped spectra showing an inflection at 0.653µm, combined with a flat spectrum longward of 0.653µm (Fig. 2A, 'pit outer centre – east'); and c) spectra at the rim which are similar to many other cerean bright spots: peak reflectance at 0.555µm and negative slopes longward of 0.555µm (Fig. 2A, 'pit rim (east)', 'pit rim (west)'). Floor spectra (Fig. 2A, 'floor') show transitions between pit and 'standard site' spectra. For further details see the appendices.

Differences in colour unit distribution with crater size and age are evident (see also section colour unit origin), e.g., when comparing Occator with the smaller crater Haulani (Fig. 3A and B). The Haulani impact event is younger (see section 'surface ages') than Occator and exhibits a large ray system and a high reflectivity floor. In contrast, Haulani's floor is more extensively covered with bluish material (Fig. 2B, 'bluish material on Haulani floor') of a wide reflectance range, whereas only a small area to its south shows brownish material. Dantu (Fig. 3C) is larger and older than Occator, showing two distinct colour units combined with complex floor morphology comprising a large central pit, widespread smooth surfaces, concentric and radial fracture systems, and flow/mass movement deposits at/near its wall. The northern floor material is brownish (cp. Fig. 2B 'central pit Dantu'), while the southern floor and its environment is spectrally bluish and darker. Peak reflectances up to 0.09 are found at Dantu (cp. Fig. 2B 'bright spot at Dantu floor'). Other craters show similar colours and morphology, though less prominent (Fig. S3). As at Occator, a number of further larger craters (e.g., Azacca, Ikapati, Anura, Gaue, and Inamahari) exhibit less prominent but similar central features. Interestingly, while bluish material is widely associated with young medium-sized craters < 100km diameter, the brightest bluish material is often linked with craters exhibiting dark ejecta material. Apparently, the freshly exposed material consists of a bright and a dark component, which both become less distinct due to impact gardening and space-weathering. However, comparably sized craters of older age do not show bluish material and no prominent central colour features but do show bright spots up to about 1 crater diameter distance to the walls. Simple bowl-shaped craters are often not spectrally uniform either. Among these, Oxo exhibits the brightest material with reflectances up to 0.16. Contrary to Occator, where bright material is found at the floor, all bright material at Oxo is found on and outside its wall (Fig. S3B, spectra in Fig. S4/5). Sites of low brightness in and near an old eroded crater show redder spectral slopes than elsewhere on Ceres (Fig. 2B 'eroded crater', Fig. 3D), pointing to an exogenous origin of the material (Daly and Schultz, 2015) (see Supplementary information).

4. Surface ages

In order to infer a relative chronostratigraphic framework of the cerean crust, we measured crater size–frequency distributions (see supplementary information 'methods') on the floors of several craters, the 'standard site', and the 'eroded crater' (Fig. S6). Formation ages of floors are: Oxo, Haulani, both geologically recent, Occator ~6.9Ma, Dantu ~46–68Ma, Urvara ~78Ma, and Azacca ~84Ma. The 'standard site' (~570Ma) is much older than the measured crater floor materials, but considerably younger than the eroded crater (~2.5 Ga). Most of the bluish and whitish material is associated with the youngest craters on Ceres.

5. Colour unit origin

In our current understanding the identified colour units are the products of internal (cryovolcanism, diapirism) and external (impact cratering, space weathering) evolution processes. Since Ceres is the largest carbonaceous chondritic-like body in the asteroid belt (Larson et al., 1979), it may be the most intact and the least stripped of primordial crustal material. Bright and bluish units are generally found at equatorial and intermediate latitudes, while they are virtually absent at high latitudes. This indicates either the source layer of these units does not exist at high latitudes or these layer(s) are too deep at these locations to be excavated by impacts. Also the general absence of young ray craters composed only of brownish material is puzzling. Younger craters of medium size are more frequent than larger ones, and their blue ejecta cover large areas. Contrary to the blue sites, impacts into brownish areas apparently do not alter the reflectance, possibly corresponding to mature grain size distribution.

At large impact basins, like Urvara and Kerwan, material mixing was apparently different from those of medium sized craters. At these basins bluish material is found infrequently and the dominant colour unit is brownish. The transition from overall spectrally red sloped material at the innermost, youngest part of Occator (cp. Fig. 2A 'pit innermost centre') to its outer deposits of bluish material, and the further moderate spectral reddening towards the older background, indicate a transient composition. Small craters were unable to expose or excavate bluish material and only contributed to brownish material stirring, unless it had been excavated and deposited earlier by larger impacts (e.g., Fig. 3B). The association of bluish material exclusively with medium sized craters suggests that these probed a layer of finite thickness. In contrast, the basin-forming impacts evidently destroyed, altered or penetrated the bluish layer. In particular, there is support for this scenario by the local distribution of the colour units in and outside the Urvara basin, which show some radial dependence but lower colour contrast.

6. Composition

We used absolute reflectance spectra to constrain the composition of the colour units, considering a wide range of geologically plausible materials related to carbonaceous chondrites (CCs). Colour spectra of the bright spots at Occator are consistent with mixtures of Mg-sulphates (kieserite), carbonates (magnesite) and phyllosilicates (phlogopite), whereby carbonates show the best global spectral matches (details in Fig. 4 and supplementary information). Due to the extended wavelength coverage of VIR compared to FC sulphates have been ruled out as the major component of the bright spots (De Sanctis et al., 2016). However, carbonates and phyllosilicates are confirmed by them; components which have been already suggested by King et al. (1992) and Rivkin et al. (2006)... For the bright bluish sites we found no compelling spectral equivalents. However, some CI1 meteorites provide overall bluish reflectance spectra coupled with low reflectances. Thus they could explain some bluish varieties of the dark material. Blue slopes can also be accentuated by the addition of magnetite to CI1 and CM2 chondrites (Cloutis et al., 2011a; Cloutis et al., 2011b). The red sloped spectra of the 'eroded crater' cannot be explained by CC's, even if they are highly space weathered, which apparently does not lead to a sharp increase in spectral slope (Moroz et al., 2004; Gillis-Davis et al., 2015). The best matching meteorite analogues of brownish material are

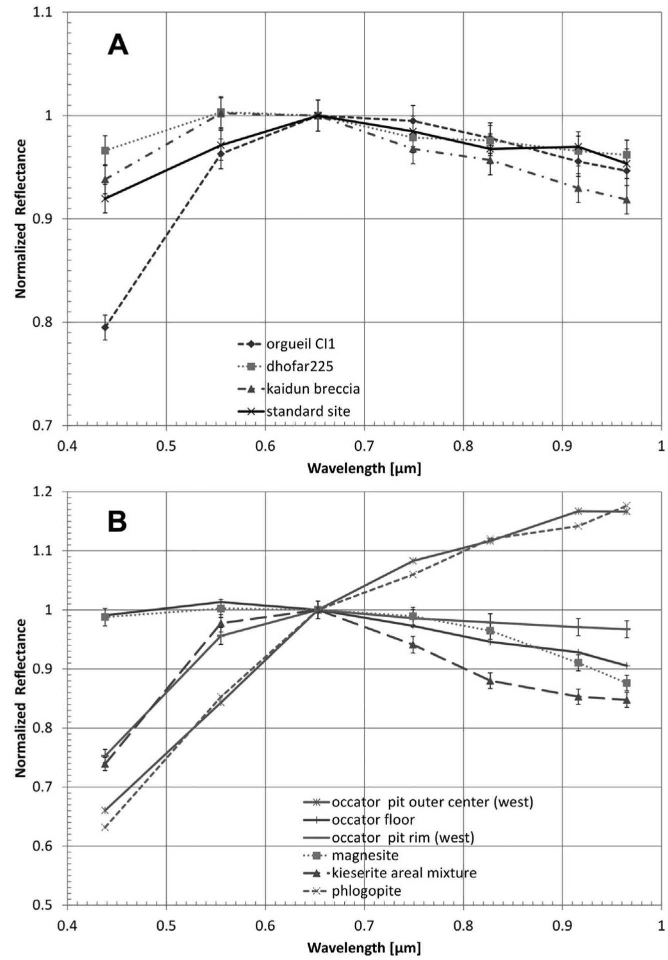

Fig. 4. Potential analogue materials of selected sites. (A) Our 'standard site' matches well with a number of CI1 meteorite spectra, both unheated and heated to between 200–400°C. (B) Occator central bright spot spectra are consistent with Mg-sulphates and standard site material mixtures (kieserite), carbonates (magnesite), and phyllosilicates (phlogopite). Error bars show standard deviation.

(Fig. 4A): (1) aqueously altered CI1 (Orgueil, and Ivuna) (Hiroi et al., 1996), and (2) CK4 chondrite ALH85002, which contains 'abundant' magnetite. Plausible candidate materials of the darkest unit are locally similar to the brownish unit: the lower reflectance can be produced by an increase in porosity, a greater abundance or more effective dispersal of dark matrix material, or enhanced space weathering. Details of our compositional analysis can be found in the supplementary information.

While the pre-Dawn notion of Ceres as a body with a surface close to CC material is consistent with our results, an unexpected dichotomy with young bluish areas has been revealed. Older craters do not show blue material. Over time this blue material can redden via a number of plausible mechanisms, including a decrease in average grain size or space weathering (Moroz et al., 2004; Gillis-Davis et al., 2015; Hiroi et al., 1996; Izawa et al., 2010; Starukhina, 2001). The blue material seems to match CI1 and modestly heated CI material (< 400°C), which are consistent with a partial differentiation of Ceres in combination with impacts, which are capable of penetrating the weathered uppermost crustal layer and delivering sufficient heat to permit localized and temporary hydrothermal processes and alteration (Hiroi et al., 1996; Izawa et al., 2010; Starukhina, 2001).

7. Stratigraphy

Based on the distribution of the identified colour units, their potential compositions, and the geomorphology of the related craters, we infer the cerean stratigraphy shown in the left-half of Fig. 5. The

Fig. 5. Sketch of Ceres' possible crustal stratigraphy at lower latitudes. Intact stratigraphy (left) and changed stratigraphy (right) by an impact demonstrating the changes of stratigraphy by exposure and re-location (layers not to scale). For craters of different size and depth the distribution changes accordingly: small craters frequently do not expose the bluish and dark units, while the deepest impacts reach deeper crustal materials (silicate and ice mixture). Occator floor material is shown on the right as darker varieties of the carbonaceous surface material that is mixed with that of the bluish and dark units. (For interpretation of the references to color in this figure legend, the reader is referred to the web version of this article.)

uppermost layer, which we have denoted as background material, is composed of carbonaceous chondritic-like material; more specifically this background material has been identified by (De Sanctis et al., 2015, 2016) to contain ammoniated phyllosilicates. Having been exposed by the impacts, we see that underneath the background material bluish and dark materials exist (i.e., as exposed at Dantu and Occator). As noted in the description of individual craters, the blue material is exclusively related to relatively young medium-sized craters, which appear to change their optical colour properties rapidly with time. The presence of water ice within the cerean crust has been confirmed by crater morphology (Hiesinger et al., 2016), flow deposit analyses (Buczkowski et al., 2016; Schmidt et al., in preparation) as well as spectral identifications of water ice at Oxo crater (Combe et al., 2016). The presence of cryovolcanism possibly triggered by impacts has been suggested (Ruesch et al., 2016) and could be responsible for the occurrence of the bright upwelling material on Occator's central-pit floor, whose reservoir is possibly a brine layer shown in Fig. 5. The lower crust finally contains possibly partially differentiated material as exposed by large impacts (e.g., Urvara basin).

8. Summary

The colours of the cerean surface are more diverse than anticipated by ground-based observations. Data obtained by the Framing Camera on-board the Dawn spacecraft led to the identification of five major colour units. The youngest of these units, the bright and bluish units, are exclusively found at equatorial and intermediate latitudes. Additionally, we identified correlations between the distribution of colour units, crater size, and formation age, and used these data to infer a cerean crustal stratigraphy. This stratigraphy explains why surface brightness and spectral properties do not correlate. The youngest surface features are the bright spots at Occator whose colour spectra are consistent with the presence of Mg-sulphates, carbonates, and phyllosilicates. While only carbonates and phyllosilicates have been identified in VIR spectroscopic data (De Sanctis et al., 2015 and 2016; Ammannito et al. 2016) the presence of sulphates is unconfirmed. Further work in progress will shed light into the detailed composition of the individual colour units. Our results demonstrate a detailed diverse geologic history of a body which has been termed before a prototype of so called “primitive asteroids”.

Acknowledgement

We thank the Dawn operations team for the development, cruise, orbital insertion, and operations of the Dawn spacecraft at Ceres. Also we would like to thank the Framing Camera operations team, especially P. G. Gutierrez-Marques, I. Hall and I. Büttner. The Framing Camera project is financially supported by the Max Planck Society and the German Space Agency (DLR).

Appendix A. Supplementary material

Supplementary data associated with this article can be found in the online version at http://dx.doi.org/10.1016/j.pss.2016.10.017.

References

Ammannito, E., et al., 2016. Distribution of phyllosilicates on the surface of Ceres. Science 353 (6303).

Buczkowski, D.L., et al., 2016. The geomorphology of Ceres. Science 353 (6303).

Castillo-Rogez, J.C., McCord, T.B., 2010. Ceres' evolution and present state constrained by shape data. Icarus 205, 443–459.

Castillo-Rogez, J.C., Choukroun, M., Hodyss, R.P., Johnson, P.V., Rivkin, A.S., Raymond, C.A., 2011. Origin of Ceres' surface as a product of mobile-lid convection. Lunar Planet. Sci. Conf. 42 (2086).

Cloutis, E.A., Hiroi, T., Gaffey, M.J., Alexander, C.M.O.D., Mann, P., 2011a. Spectral reflectance properties of carbonaceous chondrites: 1. CI chondrites. Icarus 212, 180–209.

Cloutis, E.A., Hudon, P., Hiroi, T., Gaffey, M.J., Mann, P., 2011b. Spectral reflectance, properties of carbonaceous chondrites: 2. CM chondrites. Icarus 216, 309–346.

Combe, J.-P., et al., 2016. Detection of local H_2O exposed at the surface of Ceres. Science 353 (6303).

Daly, R.T., Schultz, P.H., 2015. Predictions for impactor contamination on Ceres based on hypervelocity impact experiments. Geophys. Res. Lett. 42, 7890–7898.

De Sanctis, M.C., Ammannito, E., Raponi, A., Marchi, S., McCord, T.B., McSween, H.Y., Capaccioni, F., Capria, M.T., Carrozzo, F.G., Ciarniello, M., Longobardo, A., Tosi, F., Fonte, S., Formisano, M., Frigeri, A., Giardino, M., Magni, G., Palomba, T.B., Turrini, D., Zambon, F., Combe, J.-P., Feldman, W., Jaumann, R., McFadden, L.A., Pieters, C.M., Prettyman, T., Toplis, M., Raymond, C.A., Russell, C.T., 2015. Ammoniated phyllosilicates with a likely outer solar system origin on (1) Ceres. Nature 528 (7581), 241–244.

De Sanctis, M.C., Raponi, A., Ammannito, E., Ciarniello, M., Toplis, M.J., McSween, H.Y., Castillo-Rogez, J.C., Ehlmann, B.L., Carrozzo, F.G., Marchi, S., Tosi, F., Zambon, F., Capaccioni, F., Capria, M.T., Fonte, S., Formisano, A., Frigeri, A., Giardino, M., Longobardo, A., Magni, G., Palomba, E., McFadden, L.A., Pieters, C.M., Jaumann, R., Schenk, P., Mugnuolo, R., Raymond, C.A., Russell, C.T., 2016. Bright carbonate deposits as evidence of aqueous alteration on (1) Ceres. Nature 536, 54–57.

Gillis-Davis, J.J., Gasda, P.J., Bradley, J.P., Ishii, H.A., Bussey, D.B.J., 2015. Laser space weathering of Allende (CV2) and Murchison (CM2) carbonaceous chondrites. Lunar Planet. Sci. Conf. 46 (1607).

Hapke, B., 1981. Bidirectional reflectance spectroscopy. I. Theory. J. Geophys. Res. 86, 3039–3054.

Hapke, B., 1999. Scattering and diffraction of light by particles in planetary regoliths. J. Quant. Spectrosc. Radiat. Transf. 61 (5), 565–581.

Hapke, B., 2012. Theory of Reflectance and Emittance Spectroscopy second ed.. Cambridge Univ. Press, Cambridge, UK, (ISBN 978-0-521-88349-8).

Hiesinger, et al., 2016. Cratering on Ceres: implications for its crust and evolution. Science 353 (6303), 2016.

Hiroi, T., Pieters, C.M., Zolensky, M.E., Prinz, M., 1996. Reflectance spectra (UV-3 μm) of heated Ivuna (CI) meteorite and newly identified thermally metamorphosed CM chondrites. Lunar Planet. Sci. 27, 551–552.

Izawa, M.R.M., Nesbitt, H.W., MacRae, N.D., Hoffman, E.L., 2010. Composition and evolution of the early oceans: evidence from the Tagish Lake meteorite. Earth Planet. Sci. Lett. 298, 443–449.

King, T., Clark, R., Calvin, W., Sherman, D., Brown, R., 1992. Evidence for ammonium-bearing minerals on Ceres. Science 255, 1551–1553.

Larson, H.P., Feierberg, M.A., Fink, U., Smith, H.A., 1979. Remote spectroscopic identification of carbonaceous chondrite mineralogies applications to Ceres and Pallas. Icarus 39, 257–271.

Li, J.-Y., McFadden, L.A., Parker, J.W., Young, E.F., Stern, S.A., Thomas, P.C., Russell, C.T., Sykes, M.V., 2006. Photometric analysis of 1 Ceres and surface mapping from HST observations. Icarus 182, 143–160.

McCord, T.B., Sotin, C., 2005. Ceres: evolution and current state. J. Geophys. Res. 110, E05009.

Minton, D.A., Malhotra, R., 2009. Dynamical erosion of the asteroid belt and implications for large impacts in the inner solar system. Icarus 207, 744–757.

Moroz, L.V., Hiroi, T., Shingareva, T.V., Basilevsky, A.T., Fisenko, A.V., Semjonova, L.F., Pieters, C.M., 2004. Reflectance spectra of CM2 chondrite Mighei irradiated with pulsed laser and implications for low-albedo asteroids and martian moons. Lunar Planet. Sci. Conf. 35 (1279).

Nathues, A., Hoffmann, M., Schaefer, M., Le Corre, L., Reddy, V., Platz, T., Cloutis, E.A., Christensen, U., Kneissl, T., Li, J.-Y., Mengel, K., Schmedemann, N., Schaefer, T., Russell, C.T., Applin, D.M., Buczkowski, D.L., Izawa, M.R.M., Keller, H.U., O'Brien, D.P., Pieters, C.M., Raymond, C.A., Ripken, J., Schenk, P.M., Schmidt, B.E., Sierks, H., Sykes, M.V., Thangjam, G.S., Vincent, J.-B., 2015. Sublimation in bright spots on (1) Ceres. Nature 528, 237–240.

Petit, J.-M., Morbidelli, A., Chambers, J., 2001. The primordial excitation and clearing of the asteroid belt. Icarus 153 (2), 338–347.

Reddy, V., et al., 2012. Color and albedo heterogeneity of Vesta from dawn. Science 336, 700–704.
Rivkin, A.S., Volquardsen, E.L., Clark, B.E., 2006. The surface composition of Ceres: discovery of carbonates and iron-rich clays. Icarus 185, 563–567.
Ruesch, O., et al., 2016. Cryovolcanism on Ceres. Science 353 (6303).
Russell, C.T., et al., 2016. Dawn arrives at Ceres: exploration of a small volatile-rich world. Science 353 (6303).
Russell, C.T., Raymond, C.A., 2012. The Dawn Mission to Minor Planets 4 Vesta and 1 Ceres. Springer-Verlag, New York. http://dx.doi.org/10.1007/978-1-4614-4903-4.
Sierks, H., Keller, H.U., Jaumann, R., Michalik, H., Behnke, T., Bubenhagen, et al., 2012. The Dawn Framing Camera in: The Dawn Mission to Minor Planets 4 Vesta and 1 Ceres. Springer-Verlag, 263–327.
Starukhina, L., 2001. Water detection on atmosphereless celestial bodies: alternative explanations of the observations. J. Geophys. Res. 106 (E7), 14701–14710.